Available online at www.sciencedirect.com
ScienceDirect
Optics Communications 277 (2007) 181–185
OPTICS COMMUNICATIONS
www.elsevier.com/locate/optcom

I-scan thermal lens experiment in the pulse regime for measuring two-photon absorption coefficient

L. Rodríguez [a,*], L. Echevarria [b], A. Fernandez [c]

[a] Laboratorio de Óptica e Interferometría, Departamento de Física, Universidad Simón Bolívar, Venezuela. Caracas 1080-A, AP 89000, Venezuela
[b] Departamento de Química, Simón Bolívar, Venezuela
[c] Escuela de Química, Facultad de Ciencias, Universidad Central de Venezuela, Venezuela

Received 30 January 2007; received in revised form 18 April 2007; accepted 19 April 2007

Abstract

We present a new pump-probe mode-mismatched thermal lens method for pulse excitation aimed to the measurement of nonlinear absorption coefficient in optical materials. We develop a theoretical model based on the Fresnel diffraction approximation and their predictions are verified experimentally with samples of Rhodamine 6G and Rhodamine B in ethanol solution. The principal advantage of this technique is that it does not require any mechanical movement during measurement. Below we perform the new type of thermal lens experiment in the pulse regime for the measurement of nonlinear absorption coefficient in transparent samples and we demonstrate the validity of theoretical predictions using an alternative method to the classical thermal lens technique.

PACS: 78.20.Nv; 42.65.Jx; 42.25.Bs

1. Introduction

Due to its high sensitivity and simplicity, the pump-probe thermal lens method has been previously used in pulse regime to spectroscopy studies and the measurement of two-photon absorption (TPA) coefficients in optical materials [1–8]. In this method, the two-photon absorption by the sample from the pulsed pump beam generates temperature distributions and as consequence it induces a spatial distribution of the refraction index or thermal lens (TL). The TL induces distortions of the probe beam wave-front at the far field, which is generally measured as the change in the transmittance of a small aperture located on-axis of the probe beam. The normalized transmittance change allows to measure the TPA coefficient of the sample. Theoretical and experimental analyses of TPA were measured by TL technique and developed for first time by Twarowski and Kliger [1]. They presented theoretical and experimental results that describe the formation of TL induced by pulsed lased excitation. The thermal lens Z-scan [7,8] (TLZ-scan) technique considers diffraction effects due to the thermal lens. This method basically consists in detecting changes of the wave-fronts of a probe beam in the far field, when the nonlinear medium is scanned through the focal plane of the pulsed pump beam. The magnitude of TPA coefficient can be deduced by plotting the transmittance of a small aperture as a function of the sample position. Despite its sensitivity and experimental simplicity TLZ-scan has limitations; because this technique is both time and labor-intensive, due to a considerable number carefully TL signal measurements for each sample position are needed consuming large amounts of thermal lens signal for each sample position.

As an alternative to TLZ-scan for TPA measurements, in this work we show a simple theoretical and experimental method called I-scan thermal lens. I-scan technique consists of a typical pump-probe thermal lens experiment, however in contrast to TLZ-scan the sample is spatially fixed in the pump beam waist. The photothermal phase

* Corresponding author. Tel.: +58 2129063522; fax: +58 2129063601.
E-mail addresses: lrodigu@yahoo.com, rluis@usb.ve (L. Rodríguez).

0030-4018/$ - see front matter © 2007 Elsevier B.V. All rights reserved.
doi:10.1016/j.optcom.2007.04.034

shift is induced changing the incident intensity onto sample by means an optical attenuator. Advantages of I-scan method are: (a) simple experimental alignment, (b) none mechanical movements of the samples during the measurement and (c) high sensitivity typically observed in mode-mismatched thermal lens experiments. The proposed model is validated by measurements of two-photon cross-sections of Rhodamine 6G (Rh6G) and Rhodamine B (RhB) solutions in ethanol. The obtained results are compared with the ones reported previously.

2. Theory

Let consider us a typical pump-probe mode-mismatched TL experiment [9] in which both beams are propagating coaxially along z direction. The pump beam is used to generate the temperature distribution in the sample, as a consequence that the sample has both linear and nonlinear absorption at the pump beam wavelength; distortions in the probe beam wave-front at the far field are induced. These distortions are used to calculate the TL signal as a function of the intensity pump beam by using the Fresnel diffraction approximation. We suppose that the position of the excitation beam waist is taken as the origin of the optical system ($z = 0$) with the sample locates in this position. For a nonlinear optical material that have linear and nonlinear absorption coefficients at the wavelength of the pump beam, according to the basic TPA process, the beam intensity changes along the propagation direction z-axis and is described by:

$$\frac{\partial I(z')}{\partial z'} = -\alpha \cdot I(z') - \beta \cdot I(z')^2, \tag{1}$$

where α and β are linear and nonlinear absorption coefficients of the medium respectively, I is intensity of the pump laser and z is the spatial coordinate. By considering the thin-sample approximation the intensity distribution at the exit of the sample of thickness l may be obtained as

$$I(l) = \frac{I_0 \exp(-\alpha l)}{1 + \beta l I_0}. \tag{2}$$

In the case where $\alpha l \ll 1$ and $\beta l I_0 \ll 1$ Eq. (2) is used to determine the energy flow into unit volume per unit time at a distance r from the optical axis:

$$Q(r,t) = \frac{\Delta I}{l} = \alpha I(r,t) + \beta I(r,t)^2. \tag{3}$$

Let suppose us the pump beam is a pulsed laser with Gaussian profile in space and time:

$$I(r,t) = I_0 \exp\left(-\frac{2r^2}{w_0^2}\right) \exp\left(-4\frac{t^2}{\tau^2}\right), \tag{4}$$

where w_0 and τ are respectively the waist beam and the duration time of pulse at full width half maximum (FWHM): $\tau = \tau_p\sqrt{\ln 2}$, $w = w_0\sqrt{2\ln 2}$. The maximum on-axis intensity I_0 at the e^{-2} level is given by $I_0 = 4E/(\pi\sqrt{\pi}w_0^2\tau)$ where E is the energy of the pulse. Using the Gaussian beam described by Eq. (4) we calculate the temperature distribution of the medium solving the heat diffusion differential equation in cylindrical coordinates and assuming an infinite radial boundary condition:

$$\Delta T(r,t) = \Delta T_{01}\frac{\exp\left(-\frac{2r^2/w_0^2}{1+2t/t_c}\right)}{1+2t/t_c} + \Delta T_{02}\frac{\exp\left(-\frac{4r^2/w_0^2}{1+4t/t_c}\right)}{1+4t/t_c}, \tag{5}$$

$$\Delta T_{01} = \frac{\sqrt{\pi}\alpha I_0 D\tau}{4\kappa}, \tag{5.1}$$

$$\Delta T_{02} = \frac{\sqrt{2\pi}\beta I_0^2 D\tau}{8\kappa}, \tag{5.2}$$

where κ is the thermal conductivity, D is the thermal diffusivity and t is the time. To deduce Eq. (5) we assume that the heat generation in liquid is instantaneous. This assumption is done due to that the duration time of the laser pulse (τ), which is in the nanosecond scale range, is much less than the characteristic relaxation time associated with photo-thermal effect ($t_c = w_0^2/4D$), that is in the milliseconds scale range. The rise in temperature of the medium is accompanied by a change in its refractive index ($\Delta n = (dn/dT)\Delta T$), which alters the propagation of the probe beam. The change in the transversal phase of the probe beam ($\Delta\phi = \Delta n(2\pi/\lambda_p)l$) due to the photothermal effect is obtained by:

$$\Delta\phi(r,t) = \Delta\phi_{01}\frac{1-\exp\left(-\frac{2r^2/w_0^2}{1+2t/t_c}\right)}{1+2t/t_c} + \Delta\phi_{02}\frac{1-\exp\left(-\frac{4r^2/w_0^2}{1+4t/t_c}\right)}{1+4t/t_c}, \tag{6}$$

$$\Delta\phi_{01} = \frac{\pi\sqrt{\pi}\alpha l I_0 D\tau}{2\kappa\lambda_p}\left(\frac{dn}{dT}\right), \tag{6.1}$$

$$\Delta\phi_{02} = \frac{\pi\sqrt{2\pi}\beta l I_0^2 D\tau}{4\kappa\lambda_p}\left(\frac{dn}{dT}\right), \tag{6.2}$$

where (dn/dT) is the thermo-optic coefficient of the sample, λ_p is the wavelength of the probe beam. $\Delta\phi_{01}$ and $\Delta\phi_{02}$ are amplitudes of the photothermal phase shift due to the linear and nonlinear absorption, respectively.

The on-axis complex amplitude of the probe beam at the far field aperture is given by [9]:

$$Up(\Delta\phi(g,t)) = C\int_0^\infty [1 - j\Delta\phi(g,t)]\exp[-(1+jV)g]\,dg, \tag{7}$$

by letting:

$$g = \frac{r^2}{w_p^2}, \tag{7a}$$

$$C = j\frac{\pi w_p^2 B}{\lambda_p z_2}\exp\left(-j\frac{2\pi}{\lambda_p}z_2\right), \tag{7b}$$

$$B = \left(\frac{2P}{\pi w_p^2}\right)^{1/2}\exp\left(-j\frac{2\pi}{\lambda_p}z_1\right), \tag{7c}$$

$$V = \frac{z_1}{z_c} + \frac{z_c}{z_2}\left[1 + \left(\frac{z_1}{z_c}\right)^2\right], \tag{7d}$$

where z_1 is the distance between sample and aperture plane and z_2 is sample-waist probe beam distance. The Rayleigh range ($\pi w_p^2/\lambda_p$), the power and the radius at the sample position of the probe beam are respectively denoted by z_c, P and w_p. Placing the aperture plane in the far field ($z_2 \gg z_c$) and replacing Eq. (6) into Eq. (7) we can calculate the TL signal, which is defined as the relative change of the transmission through the small aperture:

$$\mathrm{TLS}(t) = \left|\frac{U_p(\Delta\phi(g,t)) - U_p(0)}{U_p(0)}\right|^2, \tag{8}$$

$$\mathrm{TLS}(t) = \mathrm{TLS}(t)_1 + \mathrm{TLS}(t)_{nl}, \tag{9}$$

where:

$$\mathrm{TLS}(t)_1 = \frac{4mV}{4m^2 + 4(1+2t/t_c)m + (1+V^2)(1+2t/t_c)^2}\Delta\phi_{01}, \tag{9a}$$

$$\mathrm{TLS}(t)_{nl} = \frac{4mV(1-\Phi_{\cdot\cdot tpf}\lambda_e/\langle\lambda\rangle)}{4m^2 + 4(1+4t/t_c)m + (1+V^2)(1+4t/t_c)^2}\Delta\phi_{02}, \tag{9b}$$

where sub-index 1 and nl denote linear and nonlinear, respectively. The factor $(1 - \Phi_{\cdot\cdot tpf}\,\lambda_e/\langle\lambda\rangle)$ is introduced in Eq. (9b) due to the two-photon fluorescence occurs simultaneously with generation of TL, $\Phi_{\cdot\cdot tpf}$, $\langle\lambda\rangle$ and λ_e are respectively fluorescence quantum yield, wavelength of fluorescence emission and excitation laser wavelength. The parameter $m = w_p^2/w_0^2$ was defined by Shen et al. [9] for CW laser TL technique and it is viewed as the degree of mode-mismatching of the probe beam and excitation beam in the sample. Introducing the coupling factor as the ratio of the phase amplitudes ($\Delta\phi_{02}/\Delta\phi_{01}$) in Eq. (9), we define the normalized thermal lens signal as:

$$\mathrm{NTLS} = \frac{\mathrm{TLS}(0)_{nl}}{\mathrm{TLS}(0)_1} = 1 + \frac{\sqrt{2}}{2}\frac{\beta}{l}A(1 - \Phi_{\cdot\cdot tpf}\lambda_e/\langle\lambda\rangle)I_0, \tag{10}$$

where $A = \alpha l$ is the absorbance of the sample at the pump beam wavelength, we can see that the normalized thermal lens signal is proportional to the input intensity I_0 with the proportionality factor depending on TPF quantum yield and the ratio between nonlinear and linear absorption coefficients of the sample. Eq. (10) is only valid for both $\Delta\phi_{01} \ll 1$ and $\Delta\phi_{02} \ll 1$, because thermal convective and aberrant effects are not considered in our theoretical model.

3. Experimental details and results

The experimental setup is schematized in Fig. 1. The experiments were performed with a Q-switched Nd:YAG laser (Continuum minilite) delivering 10 ns pulses at $\lambda = 1064$ nm with a repetition rate of 10 Hz. A half-wave plate ($\lambda/2$) placed before a Glan polarizer (P), allows the adjustment of the total input energy. Control of the input pulse energy is achieved by means of a beam splitter (BS_1), the reflected beam from its first surface sends about 4% of the total beam on a photodiode (D_1) connected to a two-channel digital oscilloscope. Using a positive lens (L) the beam is then focused to a spot of radius $w_0 = 200$ μm at the focal plane, corresponding to a Rayleigh length $z_0 = 12$ cm in the air. The probe beam is the light from 1-mW CW He–Ne laser ($\lambda = 633$ nm) and it passes through the sample (S), which is fixed at the waist of the excitation beam ($z = 0$). Samples consist in solutions of Rhodamine 6G (Rh6G), Rhodamine B (RhB) in ethanol, which have a concentration of 10^{-4} M contained in quartz cells of 1 cm path-lengths. A second beam splitter (BS_2) directs the probe light onto the sample in the coaxial direction of the pump beam. The interference filter (F) cancels the pump light behind the sample-cell. The probe beam finally propagates into the detection system consisting of a small aperture, ($d_0 = 1$ mm), the photodiode (D_2) and the digital oscilloscope. The two-photon fluorescence light is detected at a right angle by a collimated lens attached to the optical fiber connected to the spectrometer (Sp) (Ocean optics S2000).

Fig. 2 shows both absorbance and two-photon fluorescence spectrum of Rh6G sample indicating excitation wavelength, lineal absorbance and the emission wavelength of two-photon fluorescence, similar spectrum is obtained for RhB sample. To measure linear absorbance of samples at 1064 nm we use the typical transmittance technique from absorbance spectrum.

Analyzing absorption spectrum of Rh6G we observe that this sample has low absorption at the probe and pump beam wavelength, however only photothermal contribu-

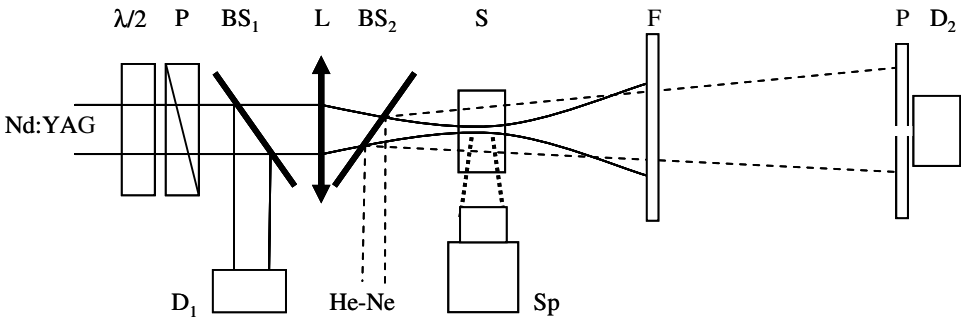

Fig. 1. I-scan experimental setup. Nd:YAG: pump beam; $\lambda/2$, P: half-wave plate and Glan polarizer; BS_i: beam splitters; D_i: photodiodes; L: positive lens; He–Ne: probe beam; S: 1 cm path-lengths sample; F: interference filter; d_0: small aperture and Sp: spectrometer.

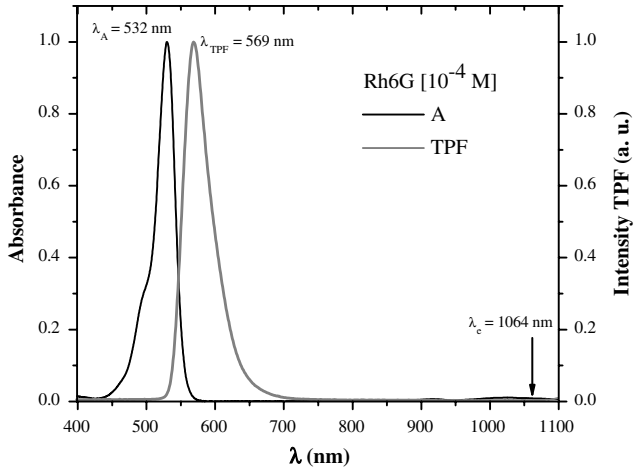

Fig. 2. Absorption and fluorescence spectra of Rh6G in ethanol solution showing wavelengths of pump beam, absorption (A) and two-photon fluorescence (TPF), respectively.

tions due to high density power of pump beam are taken into account; whereas power density of probe beam is enough low that we can neglect any thermal lens effect induced by this beam. Hence, for both tested samples the thermal lens signal is induced by absorption of one and two-photons as is predicted by Eq. (9).

We measured thermal lens and two-photon fluorescence signals as a function of the incident intensity on samples. To estimate the resolution of the measurements, a cell filled with the solvent (ethanol), was located at the waist of the pump beam and the intensity was increased from 0 to 1 GW/cm^2, neither nonlinear effects nor aberrational effects at these intensity levels were observed. In the same experimental conditions, we repeat the measurements using Rh6G. Fig. 3a shows the TLS and TPF as a function of incident intensity Io for Rh6G sample. The dependence of TLS and TPF at intensities greater than 0.6 GW/cm^2 is not considered due to aberrational effects to appear at these intensity levels. For intensities less than 0.1 GW/cm^2 the dependence TLS-Intensity shows that the photothermal effect is completely induced by the linear contribution of Eq. (9), which changes when intensity is increased revealing clearly that nonlinear process are present in the photothermal effect. This is directly verified by TPF-Intensity dependence, where typical second order slope obtained from intensities detected by the spectrometer indicates a two-photon excitation mechanism [10–12]. We measure the temporal wave-form of the laser pulse and the one on the TPF, and we obtain the FWHM of pulses are approximately 10 ns and 9 ns, respectively. This result indicates that TPF is induced from Rh6G due to a two-photon absorption process. The expected quadratic dependence of TPF on the incident density power is shown in the Fig. 3b for Rh6G sample. For the case of TLS-Intensity this second order dependence is not observed indicating that the contribution of two-photon fluorescence in Eq. (9) becomes significant to reduce the thermal lens signal.

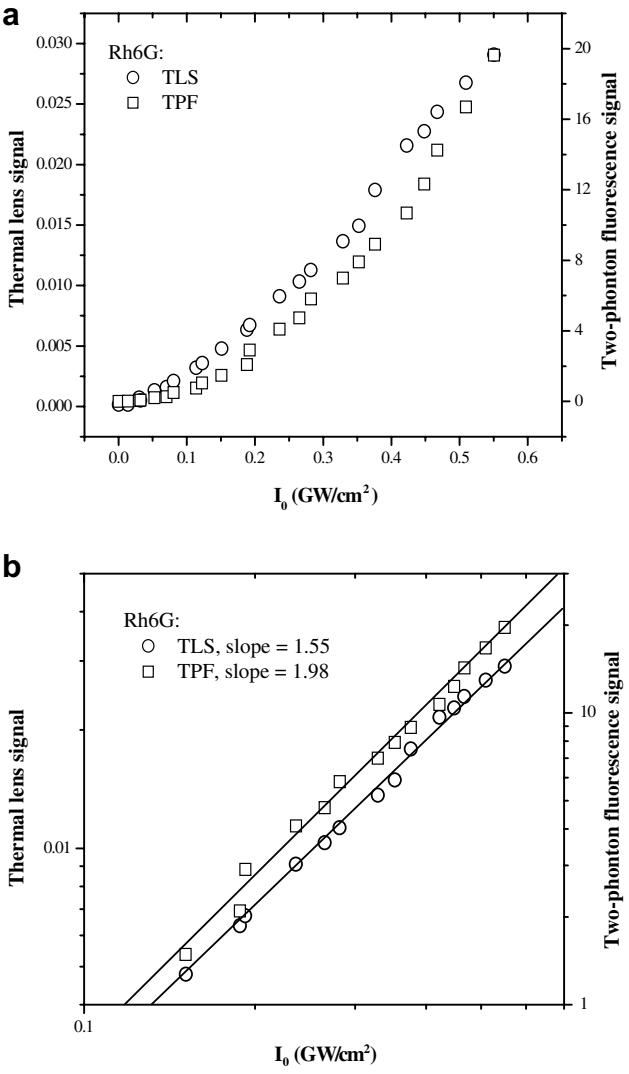

Fig. 3. (a) Experimental thermal lens and two-photon fluorescence signals as a function of the incident intensity from a 10^{-4} M of ethanol solution of Rh6G. (b) Nearly Quadratic density power dependence is observed from TPF, while, for TLS the measurement yields a slope smaller than TPF.

To determinate two-photon cross-section in Rh6G and RhB, the experimental data from TLS-Intensity dependence study were treated using the following procedure: First, the background and offset are eliminated. Second, each TLS data point was divided by its corresponding incident intensity (I_0). Finally, the results are normalized obtaining the plot shown in Fig. 4, where the calculated data as function of incident intensity verifies the linear dependence predicted by Eq. (10). This plot clearly indicates that only linear and nonlinear absorption induced the photothermal effects; neither thermal convection nor spherical aberration distortion are considering in our experiment. Linear regression fit, indicated by solid line in this figure, yields a slope with a value of 2.078 cm^2/GW. By considering this slope value and $A = 0.026$ which was previously measured by using this technique in linear regime Eq. (9a), $l = 1$ cm, $\Phi_{\text{tpf}} = 0.95$, $\langle\lambda\rangle = 569$ nm and

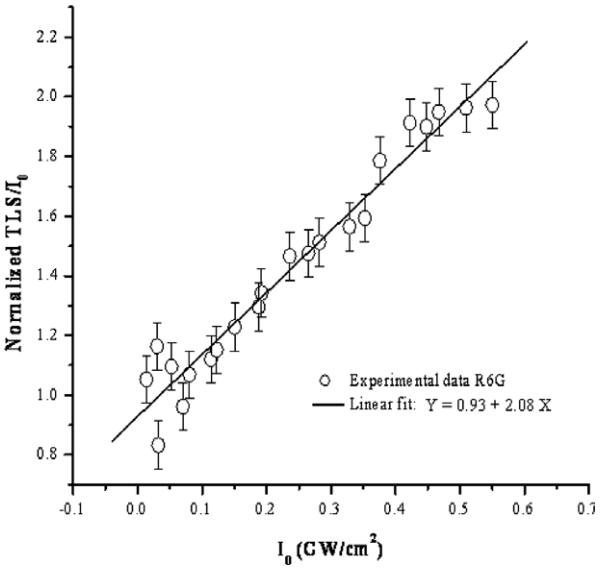

Fig. 4. Normalized thermal lens as function of incident intensity, linear function was fitted to the experimental data. The measurements agree with Eq. (10).

Table 1
Ratio of TPA cross-section (δ) of Rh6G and RhB at 1064 nm compared with other ones previously published, our obtained value of 0.95 agrees with them

	This work 2006 (10 ns)	Kaatzand Shelton 999 (125 ns)	Hermann and Ducuing 1972 (60 ns)	Bradley et al. 1972 (ns)
Rh6G/RhB	0.95	0.90	0.91	0.79

$\lambda_e = 1064$ nm as parameters for Rh6G sample, from Eq. (10) we estimate the absolute value for two-photon absorption coefficient in (0.10 ± 0.01) cm/GW. Two-photon absorption coefficient can be also expressed in term the two-photon absorption cross-section [6] $\beta = 2N\delta/h\upsilon$, where N is the number density of molecule in the sample, h Planck's constant, υ frequency of the excitation light and δ the cross-section for two-photon absorption process. The measured TPA cross-section from Rh6G is $\delta = (15 \pm 1) \times 10^{-50}\,\mathrm{cm}^4 - s$, which is comparable with the one reported by Hermann and Ducuing [10] $\delta = (12.9 \pm 6) \times 10^{-50}\,\mathrm{cm}^4 - s$ but with better precision. To determinate the compatibility of our results with the ones previous published, we calculated the ratio of two-photon absorption cross-section of Rh6G and RhB at 1064 nm. Table 1 shows the computed ratio using data reported for different author and the present work. It is clearly noticeable that our results are consistent with previously measurements at the same wavelength.

I-scan experiment and mathematical model described above are also an interesting alternative for the measurement of multi-photon absorption coefficients and the fluorescence quantum yield values with high sensitivity. Experiments are under going in order to demonstrate this important application of the proposed method. The principal advantage of the technique previously described with respect to the TLZ-scan is that it is less sensitive to the optical quality of the sample because of it does not require mechanical movements of the sample during measurements, as consequence the signal of thermal lens and two-photon fluorescence are most easily detectable.

4. Conclusion

We have developed a new theoretical and experimental model based on the Fresnel approximation for the determination of two-photon absorptions coefficients. Using this model, we have performed a comparison for different schemes of the mode-matched and mode-mismatched experiments. A comparison with previous results in the CW regime is also presented. We have proposed a new type of mode-mismatched TL experiment for the measurement of absorption with high sensitivity in the pulse regime. In this experiment the pump beam is collimated and the probe field is tightly focused. We show that this particular configuration gives larger signals comparing with the mode-matched situation and the mode-mismatched method previously reported. Extended samples can be used in this configuration in order to increase the sensitivity even further. We show the validity of the model predictions by performing absorption measurements in ethanol and toluene.

Acknowledgement

We thank the Fondo Nacional para la Ciencia y la Tecnología (FONACIT), Caracas, Venezuela, for financial support (Grant G97000593).

References

[1] A.J. Twarowski, D.S. Kliger, Chem. Phys. 20 (1977) 253.
[2] G.R. Long, S.E. Bialkowski, Anal. Chem. 56 (1984) 2806.
[3] K. Mori, T. Imasaka, N. Ishibashi, Anal. Chem. 54 (1982) 2034.
[4] R. Brennetot, J. Georges, Spectrochim. Acta Part A 54 (1998) 111.
[5] J.F. Power, Appl. Opt. 29 (1990) 52.
[6] O.A. Marcano, O.L. Rodríguez, Y. Alvarado, J. Opt. A: Pure Appl. Opt. 5 (2003) S256.
[7] V.P. Kozich, O.A. Marcano, F.E. Hernández, J. Castillo, Appl. Spectros. 48 (1994) 1506.
[8] J. Castillo, V.P. Kozich, O.A. Marcano, Opt. Lett. 19 (3) (1994) 171.
[9] J. Shen, R.D. Lowe, R.D. Snook, Chem. Phys. 165 (1992) 385.
[10] J.P. Hermann, J. Ducuing, Phys. Rev. A 5 (1972) 2557.
[11] D.J. Bradley, M.H.R. Hutchinson, H. Koetser, Proc. R. Soc. London, Ser. A 329 (1972) 105.
[12] P. Kaatz, D.P. Shelton, J. Opt. Soc. Am. B 16 (6) (1999) 998.